Obstacle Avoidance Method for AUV Based on Adaptive Fuzzy Neural Network

Jiacheng Xin[1,2], Jiwei Zhao[1,2], Kai Chen[1,2], Dong Wang[1,2], Jianguo Wu[1,2]
[1]*Tianjin Hanhai Lanfan Marine Technology Co., Ltd, Tianjin, China*
[2]*Tianjin Key Laboratory of Deep-sea Intelligent Mobile Survey Equipment, Tianjin, China*

Abstract: Aiming at the problem of autonomous obstacle avoidance of autonomous underwater vehicle (AUV) in unknown underwater environment, an adaptive fuzzy neural network obstacle avoidance algorithm is proposed, which combines the logical reasoning ability of fuzzy control and the self-learning ability of neural network. Firstly, the obstacle avoidance model of AUV in the plane is established. Secondly, the structure of the fuzzy neural network is designed. The parameters of the fuzzy membership function and the weights of the neural network are optimized by using the learning ability of the neural network, and the output error is reduced. Finally, through the simulation of AUV respectively in the horizontal plane and vertical plane within the feasibility of the proposed algorithm of obstacle avoidance.

Keywords: Furry Neural Network; AUV; Autonomous Obstacle Avoidance; Adaptive Control

1. Introduction

As an important tool for marine development, Autonomous Underwater Vehicles (AUVs) are gradually being applied in fields such as marine ranching, seabed exploration, seabed topography scanning, and coastal defense and anti-submarine warfare due to their advantages of good concealment, flexible use, and wide range of activity [1]. When navigating in complex underwater environments, autonomous obstacle avoidance capability is essential for an AUV and a crucial guarantee for the safe execution of its navigation tasks. As the requirements for the precision of AUV underwater operations become increasingly high, the autonomous obstacle avoidance technology of AUVs has gradually become a significant bottleneck restricting their intelligent development [2].

Researchers have proposed a large number of algorithms to solve the difficult problems in AUV autonomous obstacle avoidance technology [3]. Among them, the Artificial Potential Field (APF) method [4] is a typical real-time obstacle avoidance method. It was first proposed by Khatib in 1986. Its basic idea is to treat the robot's movement in the environment as motion in a virtual artificial force field, where obstacles exert a repulsive force on the robot, and the target point exerts an attractive force on the robot. The resultant force of the attraction and repulsion acts as the robot's acceleration force to control its direction of movement and calculate its position. The advantages of this method are good real-time performance, simple design, and convenient implementation. The disadvantage is the common existence of trap regions; it is difficult to find a feasible path when the AUV is among multiple obstacles or very close to an obstacle, leading to a deadlock in obstacle avoidance. Many researchers have proposed improved and optimized algorithms based on the artificial potential field method [5-7]. However, in the absence of reliable sensor equipment and effective online recognition methods for AUVs, the practical application of the artificial potential field method in AUV autonomous obstacle avoidance is subject to many limitations. In recent years, artificial intelligence algorithms have been gradually applied to AUV obstacle avoidance. The currently more common artificial intelligence methods are mainly the Fuzzy Control method [8] and the Neural Network method [9,10]. Fuzzy logic control has logical reasoning capabilities but lacks self-learning ability, while artificial neural networks have strong learning and training capabilities but lack the ability to process and describe fuzzy information [11].

This paper adopts a fuzzy neural network algorithm, utilizing the fuzzy reasoning ability of fuzzy control and the self-learning ability of neural networks, to make the entire anti-collision system's environmental adaptability more powerful.

2. AUV Obstacle Avoidance Model Analysis

2.1 Obstacle Avoidance Sonar Layout

The AUV obstacle avoidance sonar layout is shown in Figure 1. Five obstacle avoidance sonars are distributed at the bow of the AUV, and one altimeter is located directly below the bow. The forward-looking sonar and the four surrounding sonars (up, down, left, and right) have the same transmission beam angle. The altimeter's transmission beam is directed vertically downward from the AUV body to measure the AUV's altitude from the bottom during navigation. This layout can not only acquire three-dimensional spatial information about obstacles but also brings significant economic benefits compared to using forward-looking sonar.

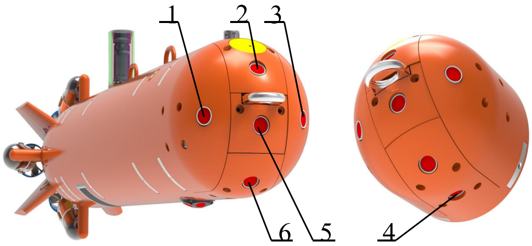

Figure 1. Obstacle Avoidance Sonar Layout
Note: 1-Forward-right sonar, 2-Forward-up sonar, 3-Forward-left sonar, 4-Altimeter, 5-Forward-looking sonar, 6-Forward-down sonar

2.2 Obstacle Distance and Shape Analysis

It is very difficult for an AUV to establish an accurate and complete three-dimensional obstacle model while navigating underwater. The propulsion system of the AUV platform used in this paper consists of four thrusters: up, down, left, and right. During navigation, the AUV changes its sailing depth by adjusting the differential speed of the upper and lower thrusters in the vertical plane, and changes its heading by adjusting the differential speed of the left and right thrusters in the horizontal plane. However, changing both depth and heading simultaneously may risk losing control of the AUV, especially when sailing at high speed with a large speed differential. Therefore, this paper analyzes obstacles by dividing them into horizontal and vertical planes based on the characteristics of the carrier's thrusters and obstacle avoidance sonar distribution, which allows for obtaining the shape and relative position information of obstacles in these two planes.

For a single obstacle avoidance sonar, only the distance between the AUV and the obstacle in that direction can be measured. However, a combination of three obstacle avoidance sonars in the same plane can not only analyze the distance to the obstacle but also obtain its shape, slope, concavity, and convexity. Figure 2 takes the horizontal plane as an example to analyze the shape features of an obstacle. In the figure, d_1 and d_2 are the distances to the obstacle detected by the forward-looking sonar and the front-left sonar, respectively.

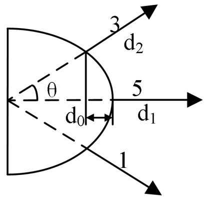

Figure 2. Bow Horizontal Sonar Arrangement

d_0 is the difference in the transducer distance of the front-left sonar and the forward-looking sonar along the central axis of the AUV. θ is the angle between the other four directional obstacle avoidance sonars and the forward-looking sonar. If

$$d_2 \cos\theta = d_1 + d_0 \tag{1}$$

then it is considered that there is a planar obstacle to the front-left of the AUV's course. Similarly, the distance information of obstacles detected by the obstacle avoidance sonars in other directions and the distance information of the obstacle detected by the forward-looking sonar can also form a rough shape of the obstacle. By integrating the distances to the obstacle obtained from the five obstacle avoidance sonars, a rough three-dimensional shape of the obstacle can be obtained. Obstacle avoidance decisions and control are then made based on the shape information of the obstacle.

2.3 Auv Obstacle Avoidance Model

The AUV's obstacle avoidance model is established in the AUV's horizontal plane two-dimensional reference coordinate system, as shown in Figure 3.

The AUV's starting position coordinates are (X_0, Y_0), the target point position coordinates are (X_g, Y_g), and the AUV's position coordinates at time t are (X_t, Y_t). Then, the AUV's position coordinates at time t+1 are (X_{t+1}, Y_{t+1}).

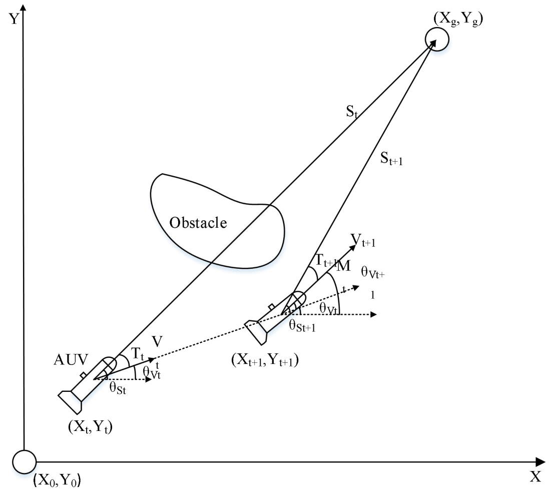

Figure 3. AUV Horizontal Obstacle Avoidance Model

The distance and angle from the AUV's position at time t to the target position are represented by the target course distance $\mathrm{S_t}$ and the target course angle θ_{St}, respectively [10]:

$$\mathrm{S_t} = \sqrt{(X_g - X_t)^2 + (Y_g - Y_t)^2} \tag{2}$$

$$\theta_{\mathrm{S}t} = \begin{cases} \arctan\dfrac{Y_g - Y_t}{X_g - X_t}, & X_g - X_t > 0 \\ \arctan\dfrac{Y_g - Y_t}{X_g - X_t} + 180°, & Y_g - Y_t \geq 0, \; X_g - X_t < 0 \\ \arctan\dfrac{Y_g - Y_t}{X_g - X_t} - 180°, & Y_g - Y_t > 0, \; X_g - X_t < 0 \\ 90°, & Y_g - Y_t > 0, X_g - X_t = 0 \\ -90°, & Y_g - Y_t < 0, X_g - X_t = 0 \\ 0°, & Y_g - Y_t = 0, X_g - X_t = 0 \end{cases} \tag{3}$$

$\theta_{\mathrm{S}t} \in (-180°, 180°]$

Assuming the AUV's sailing speed at time t is $\mathrm{V_t}$ and the heading angle is θ_{Vt}, then the AUV's sailing speed at time t+1 is $\mathrm{V_{t+1}}$ and the heading angle is $\theta_{\mathrm{Vt+1}}$. The target angle $\mathrm{T_t}$ is the angle between the AUV's target course angle θ_{St} and the current heading angle θ_{Vt} at time t. Then, the AUV's target angle at time t+1 is $\mathrm{T_{t+1}}$.

$$\mathrm{T_t} = \theta_{St} - \theta_{Vt}, \theta_{Vt} \in (-180°, 180°] \tag{4}$$

$$\theta_{\mathrm{V}t+1} = \theta_{Vt} + M_t \tag{5}$$

$$\mathrm{T}_{t+1} = \theta_{St+1} - \theta_{Vt+1} = \theta_{St+1} - \theta_{Vt} - M_t \tag{6}$$

Here, $\mathrm{M_t}$ represents the AUV's turning angle at time t, θ_{St} is calculated from the fusion of the Inertial Navigation System (INS) and the Doppler Velocity Log (DVL). θ_{Vt} is measured by the INS.

To ensure the AUV's safety during the obstacle avoidance process, setting the limit distance for avoidance is particularly important. Whether the AUV can safely bypass the obstacle and continue sailing towards the target point depends on important factors such as the AUV's current sailing speed, the overall length of the AUV, and the AUV's turning radius at the current speed. Assuming the limit distance for obstacle avoidance is S_c, its relationship with the current turning radius R_t is as follows:

$$S_c \geq R_t + l \tag{7}$$

Here, l is the overall length of the AUV, and R_t is the maximum turning radius at speed V_t at time t. Because the AUV's maximum turning radius differs at different sailing speeds, and the AUV's speed is constantly changing during its journey from the starting point to the target point, especially during obstacle avoidance when it may face deceleration, the limit distance for obstacle avoidance continuously changes with the AUV's sailing speed at different times. This avoids the problem of path redundancy caused by a single, fixed safety distance, improving the system's real-time performance and flexibility.

3. Obstacle Avoidance Algorithm Design

3.1 Fuzzy Neural Network Structure Design

By combining a BP neural network with fuzzy logic control, the characteristics of error backpropagation in the BP neural network are used to modify the weights and the center and width of the Gaussian membership function, forming a closed-loop control algorithm. The algorithm in this paper selects three single-output fuzzy neural networks to output the heading angle H, pitch angle P, and sailing speed V, respectively. The heading angle H is mainly affected by the distance information from the front-left (S_1), front-right (S_2), and forward (S_3) obstacle avoidance sonars, as well as the target angle in the horizontal direction (T_H). This network is a 4-input, single-output fuzzy neural network. The pitch angle P is mainly affected by the distance information from the forward (S_3), forward-up (S_4), and forward-down (S_5) obstacle avoidance sonars, and the target angle in the vertical direction (T_V). Therefore, this network is also a 4-input, single-output fuzzy neural network. The sailing speed V is affected by the distance information from all five obstacle avoidance sonars, making this network a 5-input, single-output fuzzy neural network.

The three networks mentioned above are all designed as 5-layer networks, with each layer having a similar function. Taking the network that outputs the heading angle H as an example, the network structure is shown in Figure 4.

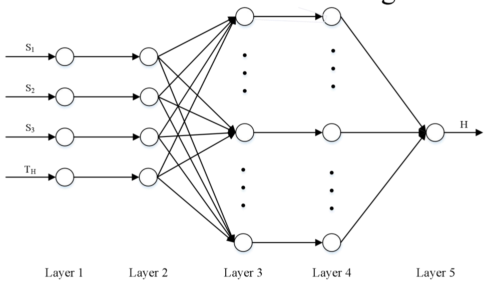

Figure 4. Fuzzy Neural Network Structure

The first layer is the input layer. The input node vector $P=[S_1,S_2,S_3,T_H]$ is composed of information about the surrounding underwater environment and heading collected by three obstacle avoidance sonars and the AUV's onboard inertial navigation system. Here, S_1, S_2, S_3 are the distance information to surrounding obstacles collected by the front-left, front-right, and forward obstacle avoidance sonars, respectively, and T_H is the angle between the AUV's current heading angle and the target heading angle. The main function of this layer is to quantify the input crisp values, transforming them from the physical domain to the fuzzy domain. By comparing with the limit obstacle avoidance distance S_c at that moment and the sonar's maximum detection distance D, the obstacle distance information, S_1, S_2, S_3 is divided into three levels: Inside the limit safety distance (I), Outside the limit safety distance (O), and the sonar's detection distance (D). The input angle is fuzzed into 7 levels: $\{NB,NM,NS,ZO,PS,PM,PB\}$. These 7 levels respectively represent the angular deviation information of the AUV's current heading relative to the target heading (Negative Big, Negative Medium, Negative Small, Zero, Positive Small, Positive Medium, Positive Big). Here, deviation to the left of the target direction is considered positive.

The second layer is the membership function layer. This layer is a hidden layer composed of 4 nodes. Its main role is to perform fuzzification on the input vector, using a Gaussian function as the conversion function to transform crisp values into fuzzy values.

$$\mu_i(x)=\exp(-\frac{(x-c_i)^2}{\sigma_i^2})\quad i=1,2,\cdots,n \tag{8}$$

Here, c_i is the center value of the Gaussian function, σ_i is the width of the Gaussian function, n is the node number, x is the input crisp value vector, and the output vector after fuzzification is $U=[\mu_1,\mu_2,\mu_3,\mu_4]$.

The third and fourth layers jointly complete the fuzzy inference process. The third layer completes the rule antecedents; the fourth layer completes the rule consequents, performing fuzzy inference and outputting a fuzzy value.

The fifth layer is the output layer. Its function is to perform defuzzification, transforming the fuzzy value from the fuzzy domain back to the physical domain.

The outputs of the three networks provide the output action space vectors for the AUV's heading angle H, pitch angle P, and sailing speed V. Here, H represents the magnitude of the AUV's horizontal turn output by the system, and H is divided into 5 levels: TLL (Turn Left Large), TL (Turn Left), TF (Go Straight), TR (Turn Right), TRR (Turn Right Large). P represents the magnitude of the AUV's vertical turn output by the system, and P is divided into 5 levels: TTU (Tilt Up Large), TU (Tilt Up), TZO (Zero Pitch), TD (Tilt Down), TDD (Tilt Down Large). V represents the magnitude of the AUV's speed output by the system, and the speed V is divided into 5 levels: FB (Fast, 4m/s), FS (Slightly Fast, 3m/s), LB (Slightly Slow, 2m/s), LS (Slow, 1m/s), ZO (Zero Speed, 0m/s). These three quantities represent the three dimensions of the output state space vector.

3.2 Fuzzy Neural Network Training Process

After determining the network structure, data from typical environments is used to train the network to determine the center and width values of the Gaussian functions, as well as the connection weights between the fourth and fifth layers. The connection weights of the other layers are set to a fixed value of 1. The network training process is shown in Figure 5.

Let the performance index function be:

$$E=\frac{1}{2}(t\arg et-output)^2 \tag{9}$$

Where, $target$ is the target output, and $output$ is the actual network output.

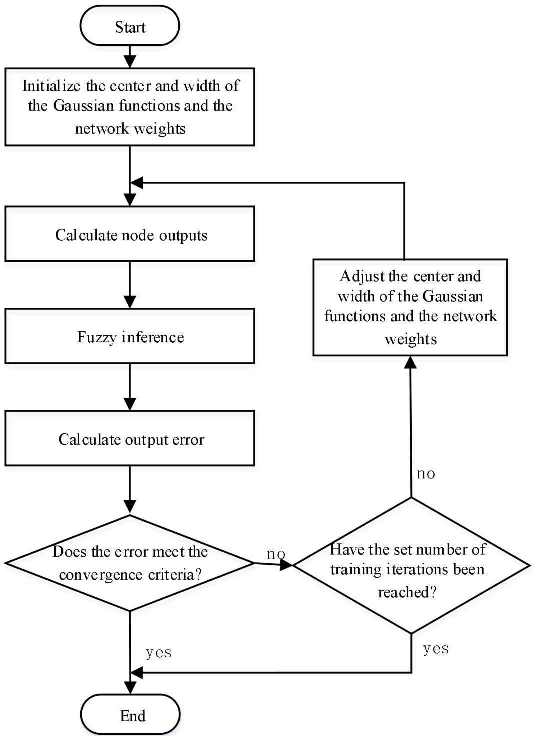

Figure 5. Fuzzy Neural Network Training Flow Chart

The network weight learning algorithm is as follows:

$$w_j^{(4)}(k+1) = w_j^{(4)}(k) + \eta_w \left[\frac{\partial E(k)}{\partial w_j^{(4)}(k)} \right] \quad (10)$$

Where, k is the sample data sequence number, $j = 1,2\cdots,n$ is the number of nodes in the fourth layer, and η_w is the learning rate.

The adjustment algorithm for the Gaussian membership function is as follows:

$$c_{i,j}(k+1) = c_{i,j}(k) + \eta_c \left[-\frac{\partial E(k)}{\partial c_{i,j}(k)} \right] \quad (11)$$

$$\sigma_{i,j}(k+1) = \sigma_{i,j}(k) + \eta_\sigma \left[-\frac{\partial E(k)}{\partial \sigma_{i,j}(k)} \right] \quad (12)$$

Where, η_c is the learning rate for c , and η_σ is the learning rate for σ .

Figure 6 shows the neural network learning curve for the heading angle H, where it can be clearly seen that the output error decreases significantly as the number of training steps increases.

4. Obstacle Avoidance Simulation

To verify the effectiveness and feasibility of the designed adaptive fuzzy neural network obstacle avoidance algorithm, a simulation is conducted. In the simulation experiment, a three-dimensional rectangular obstacle $100m \times 300m \times 50m$ is established in the coordinate system. The AUV's starting point is set to $(0m, 250m, 200m)$, and the target point coordinates are $(500m, 250m, 200m)$. The AUV's sailing speed range is simulated and set to $[0\,m/s, 4\,m/s]$. The AUV's initial heading angle in the horizontal direction is $0°$, and the pitch angle is $0°$. The maximum detection distance of the obstacle avoidance sonar is 50 m. The AUV's navigation is represented by small dots. Obstacle avoidance during navigation is controlled by the designed fuzzy neural network algorithm. The algorithm's inputs are the distance to the obstacle $[S_1, S_2, S_3, S_4, S_5]$ detected by the sonar, the angle to the target T_H in the horizontal direction, and the angle to the target T_V in the vertical direction. The algorithm's outputs are the heading angle H, pitch angle P, and speed V, respectively. H, P, and V are used to adjust the AUV's turning angle and sailing speed in real-time during the simulation. Here, for the heading angle H, 0° is parallel to the X-axis, and counter-clockwise rotation in the horizontal plane is the positive direction. For the pitch angle P, 0° is parallel to the X-axis, and counter-clockwise rotation in the vertical plane is positive. The AUV's sailing speed is represented by the distance between two adjacent dots; a smaller distance represents a slower speed, and a larger distance represents a faster speed. Finally, the curve fitted by the small dots represents the AUV's navigation trajectory.

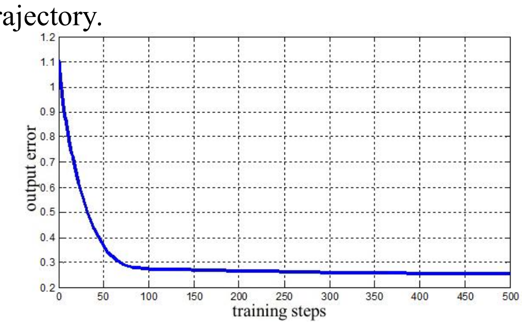

Figure 6. Neural Network Learning Curve

Figure 7 shows the AUV's obstacle avoidance trajectories in the horizontal and vertical planes during the simulation. Trajectory 1 is the avoidance trajectory in the vertical plane, and Trajectory 2 is the avoidance trajectory in the horizontal plane. It can be seen that the AUV begins obstacle avoidance at a distance of 50 m from the obstacle (the sonar's maximum detection distance). In the end, it successfully avoids the obstacle to reach the target point.

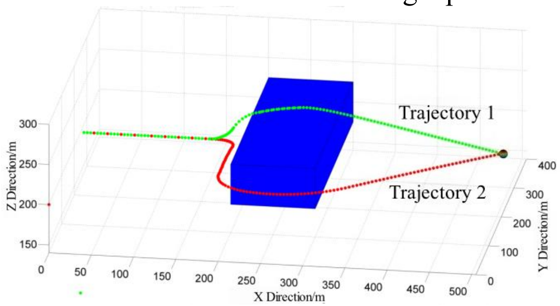

Figure 7. Obstacle Avoidance Trajectories in Horizontal and Vertical Planes

Figures 8 and 9 show the change curves of velocity V and pitch angle P with time during obstacle avoidance in the vertical plane, respectively. Figures 10 and 11 show the change curves of velocity V and heading angle H with time during obstacle avoidance in the horizontal plane, respectively. It can be seen that when an obstacle is detected, the control algorithm automatically adjusts the speed and the pitch or heading angle. This enables the avoidance of the obstacle. After avoiding the obstacle, the speed returns to its maximum, and the pitch or heading angle points towards the target.

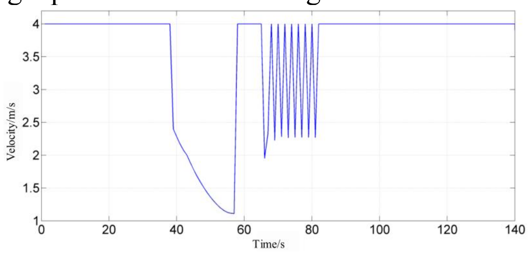

Figure 8. Curve of Obstacle Avoidance Velocity in Vertical Plane with Time

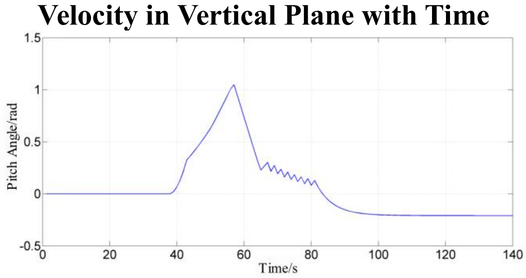

Figure 9. Curve of pitch angle of obstacle avoidance in vertical plane with time

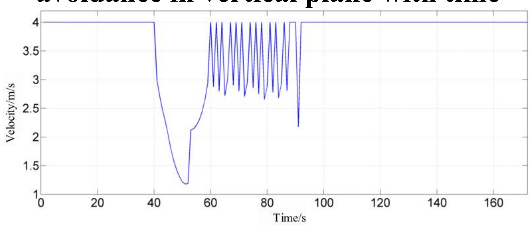

Figure 10. Curve of Obstacle Avoidance Velocity in Horizontal Plane with Time

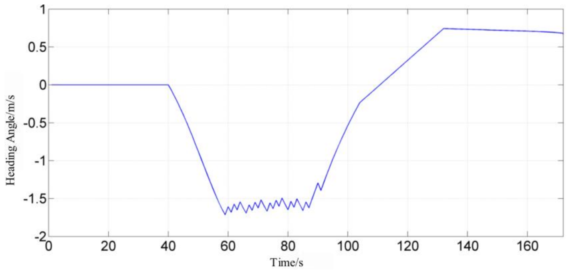

Figure 11. Curve of Heading Angle of Obstacle Avoidance in Horizontal Plane with Time

5. Conclusion

This paper addresses the problem of autonomous obstacle avoidance for an AUV in an unknown underwater environment. It proposes an autonomous obstacle avoidance control algorithm based on a fuzzy neural network. The algorithm uses three single-output fuzzy neural networks to control the three dimensions of the AUV's navigation and obstacle avoidance process. The algorithm combines the advantages of fuzzy control and neural networks, making the AUV's autonomous obstacle avoidance process more intelligent. The simulation results show that the autonomous obstacle avoidance control algorithm based on the fuzzy neural network, by coordinately controlling the sailing speed V, heading angle H, and pitch angle P, can achieve obstacle avoidance for the AUV in both horizontal and vertical planes within an unknown underwater environment. In a real marine environment, an AUV's navigation is affected by many factors. This paper only verified the feasibility of the algorithm in an ideal simulation environment. Therefore, the next step requires testing the algorithm in a real-world environment.

References

[1]Zheng Zeng, Lian Lian, Karl Sammut, Fangpo He, Youhong Tang, Andrew Lammas. A survey on path planning for persistent autonomy of autonomous underwater vehicles. Ocean Engineering,2015,110.

[2]Guo Yiping, Wang Yimin, Ren Yuanzhou. Research on AUV Trajectory Tracking Control Technology Based on Line-of-Sight Guidance Method. Acoustics and Electronics Engineering, 2018(04):32-36+40. (in Chinese)

[3]Yao Peng, Xie Zexiao. An AUV Autonomous Obstacle Avoidance Method

Based on Modified Navigation Vector Field. Acta Automatica Sinica:1-11(2019-02-19). (in Chinese).
[4]Johann Borenstein, Yoram Koren.Real-time avoidance for fast mobile robots. IEEE Transactions on Systems, Man and Cybernetics,1989, 19(5):1179-1187.
[5]Yang Jian, Meng Fanchen. Research on Obstacle Avoidance Motion Method for Micro AUV Based on Artificial Potential Field Method. Mine Warfare and Ship Protection, 2017, 25(04):67-71. (in Chinese)
[6]Xing Mingzhi. Research on AUV Planning and Obstacle Avoidance Method Based on Fish Swarm-Artificial Potential Field Algorithm. Harbin Engineering University, 2024. (in Chinese)
[7]Pan Yunwei, Li Min, Zeng Xiangguang, et al. Obstacle Avoidance and Path Planning for Autonomous Underwater Vehicle Based on Artificial Potential Field and Improved Reinforcement Learning. Acta Armamentarii, 2025, 46(04):72-83. (in Chinese)
[8]Xu Hongli, Feng Xisheng. Research on AUV Fuzzy Obstacle Avoidance Method Based on Event Feedback Monitoring. Proceedings of the Conference on Automation and Advanced Integration Technologies (II), 2007:704-708. (in Chinese)
[9]Yu Jiancheng, Zhang Aiqun, Wang Xiaohui, Su Lijuan. Direct Adaptive Control for Underwater Robot Based on Fuzzy Neural Network. Acta Automatica Sinica, 2007(08):840-846. (in Chinese)
[10]Zhang Yibo, Gao Bingpeng. Research on AUV Path Planning Based on Deep Reinforcement Learning. Journal of Northeast Normal University (Natural Science Edition), 2025, 57(01):53-62. (in Chinese)
[11]Kong Lingwen, Li Pengyong, Du Qiaoling. Design of Closed-loop Control System for Autonomous Navigation of a Hexapod Robot Based on Fuzzy Neural Network. Robot, 2018, 40(01):16-23. (in Chinese)
